JOURNAL OF OPTOELECTRONICS AND ADVANCED MATERIALS Vol. 9, No. 11, November 2007, p. 3522 - 3528

Performance of the Howard University Raman Lidar during 2006 WAVES campaign

M. ADAM[a*], D. VENABLE[a], R. CONNELL[a], E. JOSEPH[a], D. N. WHITEMAN[b], B. B. DEMOZ[a,b]
[a] *Howard University, Washington, DC 20059, USA*
[b] *NASA/Goddard Space Flight Center, Greenbelt, MD 20771, USA*

The WAVES 2006 field campaign took place at the Howard University Research Campus in Beltsville, MD, USA during July and August. The field campaign was mainly intended to provide quality measurements of water vapor and ozone for comparison with AURA satellite retrievals. The operations include intensive observations by multiple radiosondes sensors and several lidar systems during overpasses of the AURA satellite. The Howard University Raman Lidar system operates at the third harmonic of a Nd:YAG laser and acquires data at 354.7 nm, 386.7 nm and 407.5 nm. The present study shows the temporal and spatial retrievals of the water vapor mixing ratio as well as comparisons of individual profiles with radiosondes and NASA/GSFC Scanning Raman Lidar system.

(Received August 1, 2007; accepted November 1, 2007)

Keywords: Raman Lidar, WAVES, Howard University

1. Introduction

The WAVES (Water Vapor Variability – Satellite/Sondes) 2006 field campaign took place at the Howard University Research Campus in Beltsville, MD, USA from July 7 to August 10. The field campaign was intended to provide quality measurements of water vapor and ozone for comparison with AURA satellite retrievals and to quantify the air quality [1]. The operations include intensive observations by multiple radiosonde/ozonesonde sensors and several lidar systems during overpasses of the AURA satellite. Lidar measurements are acquired by four lidar systems: NASA/GSFC Scanning Raman Lidar (SRL), NASA/GSFC Aerosol/Temperature Lidar (ATL), a Micropulse Lidar from Penn State University and Howard University Raman Lidar (HURL). Coordinated lidar measurements took place as well at University of Maryland, Baltimore County (backscatter and Raman lidars) in order to provide information about the spatial variability of the aerosol and water vapor. In addition to the lidar/radiosondes operations, continuous measurements are taken by a 31 m instrumented tower (for temperature, flux, wind etc), various broad-band and spectral radiometers, microwave radiometer, Doppler C-band radar, various aerosol chemical parameters, wind profiler (operated by the Maryland Department of Environment) as well as by a sun photometer, and a Suominet GPS system.

The HURL system operates at the third harmonic (typical operating power is 10 W) of an Nd:YAG laser and acquires data within three channels, at 354.7 nm (elastic backscatter and pure rotational Raman respectively), 386.7 nm and 407.5 nm (Raman scattering from nitrogen molecules and water vapor molecules). Eye-safety is accomplished by means of a 15X beam expander. The laser beam and telescope divergences are 50 μrad and 250 μrad respectively. The telescope has a diameter of 0.4 m. The data acquisition is achieved with Licel Transient Recorders which allow both photon counting and analog acquisition. The combination of both methods ("gluing") gives maximum dynamic range. For the data processing, the following corrections are applied: response time correction, dark-current and background subtraction, and noise reduction [2]. The first data of the HRL system were acquired in 2004 and the WAVES experiment is the first major participation within a field campaign aimed at intra-lidar comparison.

The present paper shows temporal and spatial retrievals of the water vapor mixing ratio (WVMR) and few examples of HURL comparisons with RS92 and SRL. Preliminary results show good agreement between HURL and SRL systems throughout the useful range of water vapor profiles on one hand and between HURL and radiosondes (RS92) profiles on the other hand.

2. Lidar data processing methodology

2.1 Lidar gluing procedure

Combination of analog (AD) and photon counting (PC) signals allows us to use the analog data in the strong signal regions and the PC data in the weak signal regions. The idea is to form ordered pairs of (AD, PC) data in a region where both are considered to be performing in a reasonably linear fashion and perform a regression. Prior to the regression, the photon counting data are corrected for pulse pileup using a non-paralyzable assumption. The regression determines the gain coefficient that is then used to convert the AD scale to a "virtual" photon countrate scale [3]. First, the gluing coefficients are determined profile by profile by regression (at least 25 points are used in regression) after background subtraction (red, green and blue curves in Fig. 1 represent the gluing coefficients for aerosol, nitrogen and water vapor respectively). In the second step, the mean gluing coefficients (for each of

aerosol, nitrogen and water vapor) are determined (see the thick lines in Fig. 1). Few criteria are involved in determining the mean gluing coefficients. First, only profiles with a regression correlation coefficient R2 larger than 0.99 (aerosol), 0.99 (nitrogen) and 0.97 (water vapor) are selected. A mean and standard deviation (STD) are calculated for R2. Profiles outside the boundaries defined by mean ± STD for R2 are eliminated. For the remaining profiles, the mean and STD are computed for the gluing coefficients. Further, profiles lying outside the boundaries defined by the mean ± STD for gluing coefficients are excluded. The remaining set of profiles determines the final mean gluing coefficients. The criteria involved assure us to exclude outliers when determining the mean gluing coefficients.

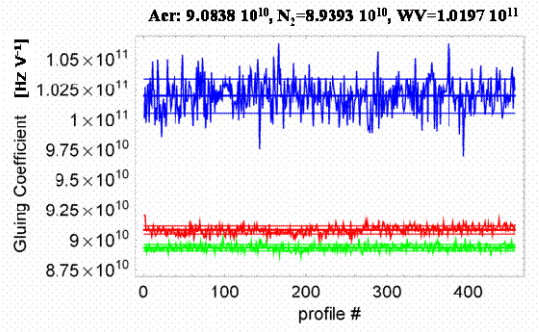

Fig. 1. Gluing coefficients for August 12, 00:05 - 07:42 UT. The red, green and blue curves represent the gluing coefficients for aerosol, nitrogen and water vapor respectively. Also shown, the mean (thick lines) and mean ± STD (thin lines). The values of the mean gluing coefficients for aerosol, nitrogen and water vapor channels are given on top of the graph in units of Hz V^{-1}.

2.2 Water vapor mixing ratio equation

The WVMR is defined as the ratio of the WV and dry air masses, where the individual mass is the product of the number of molecules and molecules' molecular weight. The number of water vapor molecules and dry air molecules are determined from the Raman signals corresponding to water vapor and nitrogen channel. The final expression can be written as [4]:

$$w = Ck\frac{O_N(r)}{O_H(r)}\frac{F_N\left[T(r)\right]}{F_H\left[T(r)\right]}\frac{P(\lambda_H,r)}{P(\lambda_N,r)}\Delta\tau(\lambda_N,\lambda_H,r) \qquad (1)$$

where $P(\lambda_H,r)$ and $P(\lambda_N,r)$ are backscattered power (after background subtraction) at 354.7 nm and 386.7 nm, $O_N(r)$ and $O_H(r)$ are the overlap functions for nitrogen and water vapor channels, $\Delta\tau(\lambda_N,\lambda_H,r)$ is the differential transmission defined as [4]:

$$\Delta\tau(\lambda_N,\lambda_H,r) = \exp\left\{-\int_0^r\left[\alpha(\lambda_H,r')-\alpha(\lambda_N,r')\right]dr'\right\} \qquad (2)$$

where $\alpha(\lambda_H,r)$ and $\alpha(\lambda_N,r)$ are the extinction coefficients at water vapor and nitrogen Raman shifts. Functions $F_N[T(r)]$ and $F_H[T(r)]$ are introduced to carry the temperature dependence of the lidar equations [5] and in practice they can be computed as:

$$F_X\left[T(r)\right] = \sum\frac{d\sigma_X(\lambda',\pi,T)}{d\Omega}\xi(\lambda')d\lambda' \qquad (3)$$

having units of m^{2}sr^{-1}; $d\sigma_X(\lambda,\pi,T)/d\Omega$ is the differential backscatter cross-section and $\xi(\lambda)$ is the filter transmission; X stands for either nitrogen N or water vapor H. The numerical value C≅0.485 comes from the ratio of water molecular weight to dry air molecular weight multiplied with 0.78 (~ percentage of nitrogen in the air). The constant k accounts for other optical efficiencies, like reflectivity of the telescope, transmission of conditioning optics and quantum efficiency of the detector.

2.3. Incomplete overlap correction

In the WVMR equation (1) the ratio of the nitrogen overlap function to the water vapor overlap function might not be unity in the region of the incomplete overlap. In order to extract useful information from that region, a correction has to be applied. In the present study, a correction function was determined from the ratio of the WVMR from lidar and radiosondes (RS92) profiles [3]. Eight sets of profiles were chosen over the entire experiment period. The individual ratios as well as their mean are shown in Fig. 2 (a). An analytical function was defined to match the experimental mean [Fig. 2(b)]. The fit for the mean ratio is determined as a polynomial function of degree 9 as a function of exp(-h), where h is the height (altitude). As seen from the figure, the correction function ranges over first ~ 1400 m and not considering such correction leads to errors in the WVMR of about 15 % at ~ 400 m and ground level.

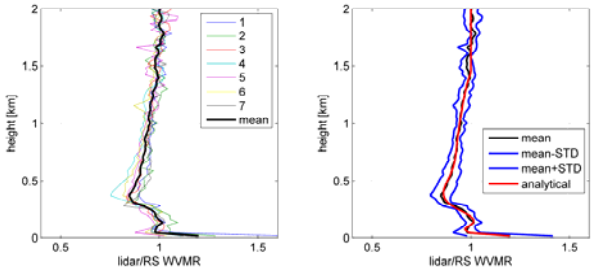

Fig. 2. (a) Individual and mean ratios of lidar to RS92 WVMR. (b) Mean and STD and the analytical fitting.

2.4 Lidar water vapor mixing ratio calibration

The differential transmission term $\Delta\tau(\lambda_N,\lambda_H,r)$ is computed using radiosondes pressure and temperature measurements to account for the molecular attenuation and

a constant aerosol extinction coefficient over BL, derived from the Aeronet [6] aerosol optical depth and the length of the boundary layer (BL) height to account for aerosol attenuation. The temperature dependence of the lidar signals are computed according to eq. (3).

The lidar calibration for WVMR is performed by comparison of the lidar integrated precipitable water (IPW) with the microwave radiometer (MWR) IPW data for night time periods [3]. The lidar profile for WVMR is first corrected for the region of incomplete overlap. Due to the increased noise with the range for the lidar signals, the IPW above altitudes of 8 km is calculated from radiosondes WVMR data, accounting for approximately 1 - 2 % of the total IPW as measured by MWR. The MWR to lidar IPW ratio gives the lidar calibration constant for WVMR. In Fig. 3 (August 12, 2006), the individual calibration points are shown by black curve. Initially, the mean and the STD are computed. The outliers outside the boundaries defined by STD = ± 5 % of the mean are excluded. With the remaining set of points, a new mean and STD are computed (red and green lines in Fig. 3). For this particular set of data, the mean calibration is 345.2 g/g while its STD is 4.76 g/g.

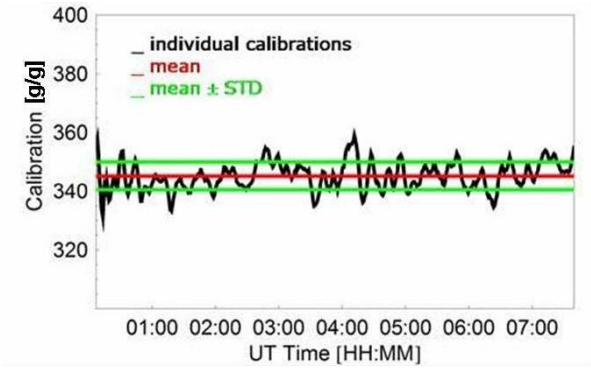

Fig. 3. The calibration constant given by the IPW ratio of MWR to lidar for 12 August, 2006. Mean and STD are 345.2 g/g and 4.76 g/g, respectively.

3. Results

3.1 Radiosondes comparisons

The lidar profiles are interpolated at the time and height of RS92 (tracking the RS) (e.g. Fig. 4, for August 12, 6:01 UT RS launch time). The technique was discussed by Whiteman et al. [7] during AVEX campaign. The only assumption is that the atmosphere is horizontally homogeneous, to account for possible horizontal shifts in the RS trajectory. A moving average was performed over 5 temporal profiles (5 min) and over 5 altitudes bins (150 m).

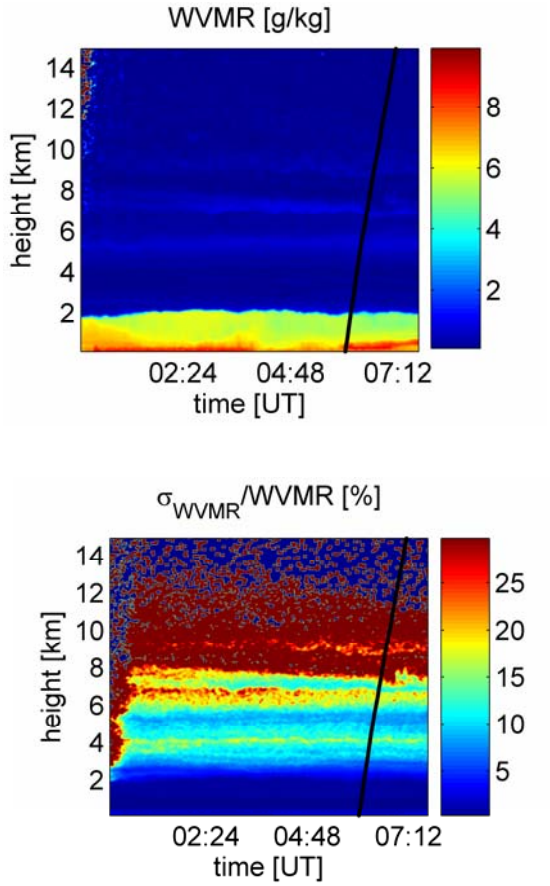

Fig. 4. Example of tracking the radiosonde. The left plot represents WVMR while the right plot represents the relative error (σ_{WVMR}/WVMR). The RS launch time was 6:01 UT on August 12, 2006. The black curve represents the RS trajectory.

The radiosondes comparisons within this study were performed with respect to NASA/GSFC RS92 radiosondes. Below we show few comparisons for night time periods. A moving average over five minutes (five profiles) in time and over five bins (150 m) in altitude was performed. The first example is a comparison from July 11 (RS92 launch time: 6:05 UT). The met tower WVMR at 1.5 m and 31.8 m are 14 and 15.7 g kg^{-1} respectively. Fig. 5 shows the lidar and RS92 WVMR profiles on the left plot and the relative differences between RS92 and lidar profiles on the right plot. A second example is from July 20 (RS92 launch time: 5:54 UT) (Fig. 6). The met tower WVMR at 1.5 m and 31.8 m are 18.7 and 17.7 g kg^{-1}. The final example is from August 12 (RS92 launch time: 6:01 UT) (Fig. 7). The met tower WVMR at 1.5 m and 31.8 m are 10.3 and 9 g kg^{-1}. In all examples, a moist bias can be observed for the RS profiles. Accordingly the relative differences increase. Disregarding the bias, a good agreement is met for the first ~ 3 km.

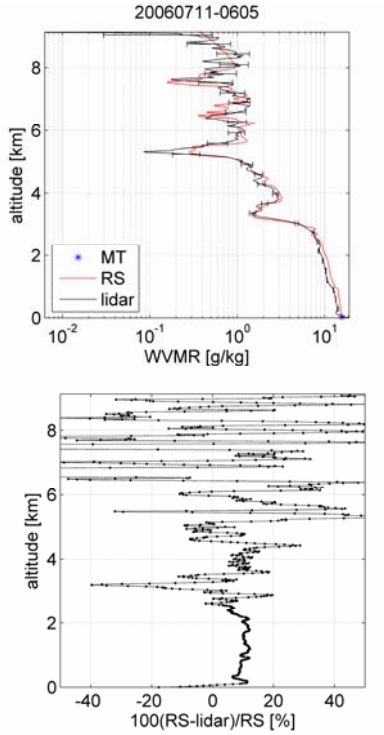

Fig. 5. RS92 and lidar WVMR profiles (red and black curve respectively), the met tower WVMR at 1.5 m and 31.8 m (14 and 15.7 g kg^{-1}, blue dots) (left plot). The relative differences between RS92 and the lidar profile.

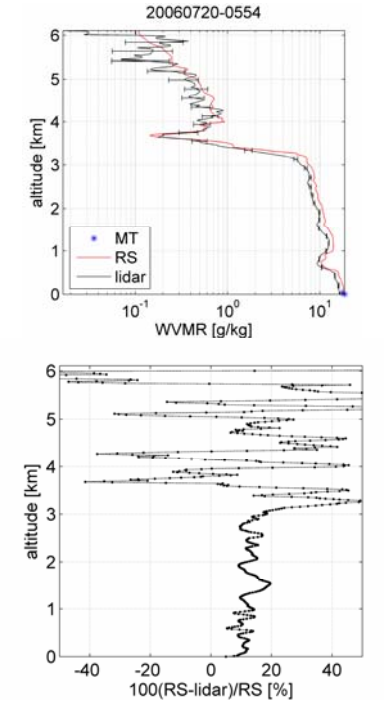

Fig. 6. RS92 and lidar WVMR profiles (red and black curve respectively), the met tower WVMR at 1.5 m and 31.8 m (18.7 and 17.7 g kg^{-1}, blue dots) (left plot). The relative differences between RS92 and the lidar profile.

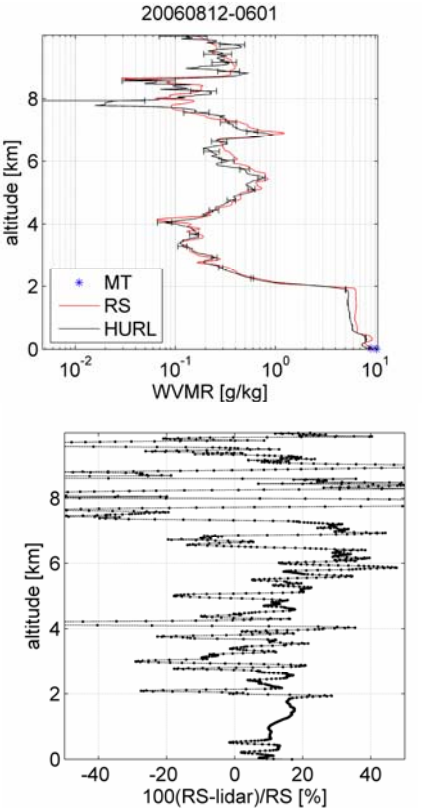

Fig. 7. RS92 and lidar WVMR profiles (red and black curve respectively), the met tower WVMR at 1.5 m and 31.8 m (10.3 and 9 g kg^{-1}, blue dots) (left plot). The relative differences between RS92 and the lidar profile.

Ensemble average ("the value of a meteorological variable found by averaging over many independent descriptions or realizations of that variable") over 10 data sets reveals the bias between RS92 and HURL (Fig. 8) within first 2 km. While differences between mean HURL and mean RS92 at high altitudes can be correlated with larger STD for RS92 or HURL (random errors), the difference over the first 2 km can be correlated with systematic errors (e.g. RS92 moister within the PBL).

3.2. SRL-HRL comparisons

The SRL system operated also at the third harmonic (~ 10 W) of an Nd:YAG laser, acquired data at 354.7 nm, 386.7 nm and 407.5 nm, had a frequency of 30 Hz and used PC and AD acquisition. In addition, it measured also, depolarization and liquid water content and it has two telescopes for receiving the backscatter signals: 25 cm (high channel) and 76 cm (low channel). The SRL was a well established instrument in the lidar community with a rich history of making successful measurements of tropospheric water vapor (e.g. [3], [7]-[11]).

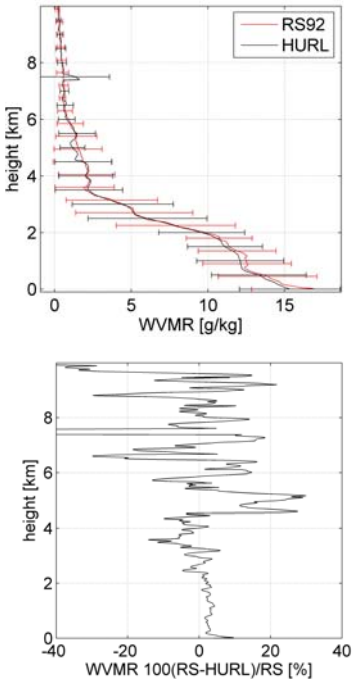

Fig. 8. Ensemble average over 10 profiles (taken over the period July 11 – August 12, 2006).

A temporal moving average over 5 profiles (5 min) and a variable moving average over height were used for both lidars data. Fig. 9 shows a HURL-SRL-RS92 comparison for August 12th. The right panel represents the relative block average (average over blocks of 1 km altitude) difference with respect to RS92.

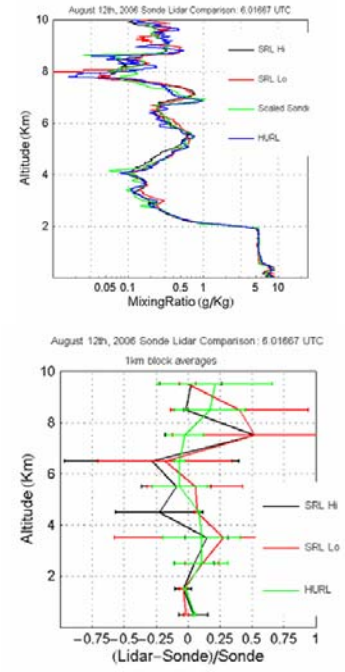

Fig. 9. HURL-SRL-RS92 comparison for Aug. 12th. The right plot shows a block average difference between RS92 and lidars.

Fig. 10 shows comparison of the lidars as 2-hour averages for the interval 7 - 9 UT. The right plot shows the relative difference wrt HURL. HURL – SRL comparison shows agreement within 10 % within the first 6 km with both high and low SRL channels.

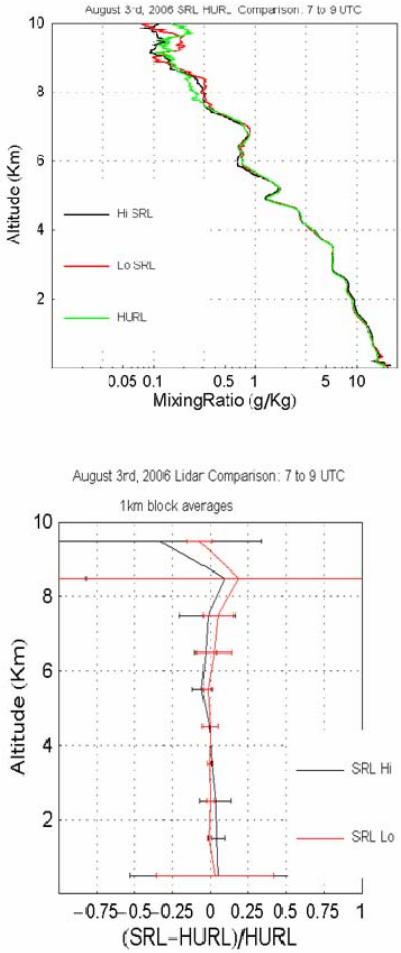

Fig. 10. Lidars two-hour WVMR averages for Aug. 3rd, 7-9 UT (left plot) and the relative difference wrt HURL (using block averages over 1 km) (right plot).

Fig. 11 shows the time series of WVMR for HURL and SRL (high channel) for August 3rd, 2006 [(a) and (b)], the time series of the WVMR relative error (STD/mean) for both lidars [(c) and (d)] and the relative difference wrt HURL of the mean profiles [(e)]. For SRL lidar, the height up to where the relative error is less than 10 % is slightly higher than HURL's. Roughly, both systems have a relative error less than 10 % up to 5 – 6 km during night-time and up to 3 – 4 km during day-time. The relative difference of the two lidars is correlated with the relative errors of the systems. In other words, the WVMR from both systems agrees well up to 6 – 8 km during night-time and 4 km during day-time.

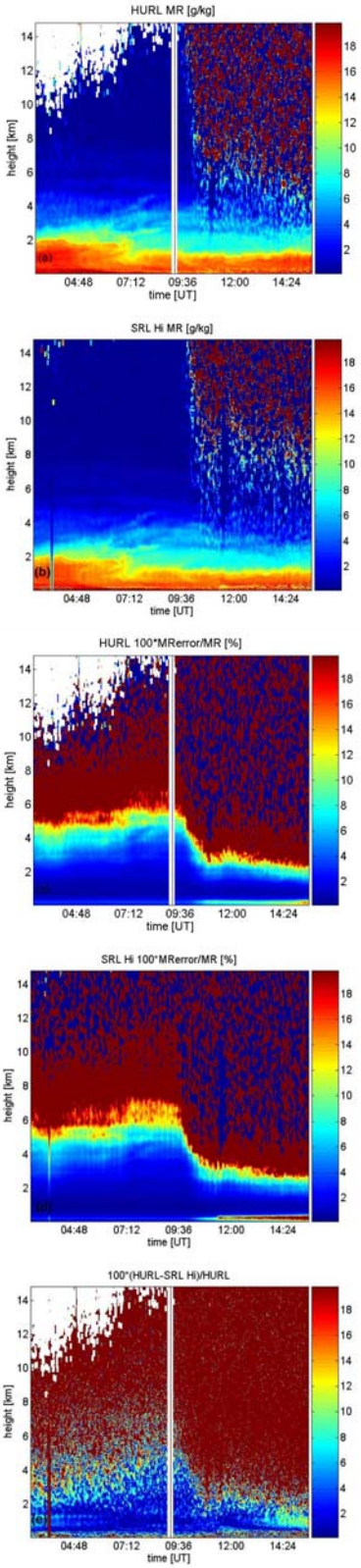

Fig. 11. Time series of WVMR for HURL and SRL (high channel) for August 3rd, 2006 [(a), (b)], time series of the WVMR relative error (STD/mean) for both lidars [(c), (d)] and the relative difference wrt HURL of the mean profiles [(e)].

4. Discussion

The HURL system is able to determine the WVMR within 10 % relative error or better from ground to 4 -10 km during night (e.g. Figs. 4-11) and from ground to 4 - 6 km during day (Fig. 11). However, improvement of the statistical errors will be performed in the future studies by using variable averaging in time and space to achieve relative errors within 10 % up to the upper troposphere. The first comparisons with collocated SRL system show reasonable results (Fig. 11). The routine comparisons of the lidar WVMR profiles with radiosondes WVMR profiles reveal more or less significant differences. This issue has been a matter of investigation in the last decade and it is still under investigation (e.g. [7], [8]). In the present study, the RS shows a moist bias with respect to HURL profiles. We mention that currently, various RS92 corrections are underway and comparisons with Cryogenic Frostpoint Hygrometer relative humidity sensors [8] are performed.

In the near future, we will focus within the potential sources of errors. At this time we are aware of the following sources of errors which are propagated within the calculation procedure: gluing procedure, RS92 WVMR precision, correction function for the incomplete overlap region (it is directly influenced by the precision of the RS profile); calibration constant (directly influenced by the accuracy of the incomplete overlap correction function as well as by the smoothing/averaging techniques). The gluing coefficients may vary during measurements period and the option of using a mean gluing coefficient in the final gluing step may induce errors within few percentages in certain cases. So far, our analyses reveal sometimes differences within 5 % between an individual gluing coefficient and the mean, which is equivalent with a 5 % change in the backscatter signal. During next 2007 WAVES campaign, a direct determination of the individual overlap functions for the HURL system is envisaged. The lidar profiles of thee ground based HURL system will be directly compared with the airborne NASA/GSFC Raman Aerosol Scanning Lidar (RASL) system. The incomplete overlap correction, performed independent of RS allows the lidar to play an important role in various corrections applied to RS itself. The use of a mean calibration constant (similar with the use of a mean gluing coefficient) can induce error as well in the WVMR within few percents. Within this context, a small error in the precision can be critical for meteorological modeling. A thorough analysis is envisaged in order to reveal the causes behind the slight variation of the gluing coefficients as well as the calibration constant. Nonetheless, a special attention will be given on the process of error propagation, particularly by including other errors besides random errors described by Poisson statistics. The analysis of the

systematic errors is a challenge but it is crucial in determining the accuracy of our results.

5. Conclusions

The first RS92-HURL comparisons along with SRL-HURL comparisons for WVMR show promising results. Good comparisons usually are met on the BL region where the WVMR values are large. As we go up, above the BL region, the WVMR decrease substantially. Consequently, the relative difference between two small quantities will result in large percentages. However, a bias exists between RS92 and HURL (RS92 moist). The relative difference between RS92 and HURL is comparable with the relative difference between RS92 and SRL. HURL – SRL comparison shows a good agreement within 10 % within first 6 km with both high and low SRL channels. Within this context, the HURL system is shown to be capable of acquiring qualitatively good data during both nights and days periods. Next studies envisage the HURL WVMR comparisons with Tropospheric Emission Sounder and The Advanced Infrared Sounder sensors on AURA and AQUA satellite respectively. Comparison of HURL results with both radiosonde and SRL results demonstrates the value of HURL as a well qualified instrument for making water vapor mixing ratio measurements in the lower troposphere.

Unfortunately, the SRL system was severely damaged in transit to a field campaign in October 2006. However, it will be replaced by a new system (ALVICE).

This work was supported in part by NASA and by NOAA.

References

[1] D. N. Whiteman, M. Adam, B. Bojkov, B. Demoz, J. Fitzgibbon, R. Forno, R. Herman, R. Hoff, E. Joseph, E. Landulfo, K. McCann, T. McGee, L. Miloshevich, I. Restrepo, F. Schmidlin, B. Taubman, A. Thompson, D. Venable, H. Vomel, C. Walthal, 7th International Symposium on Tropospheric Profiling, Boulder, CO (2006). (http://www.eol.ucar.edu/istp2006/istpprogram.html)

[2] D. Venable, E. Joseph, D. N. Whiteman, B. Demoz, R. Connell, S. Walford, The development of the Howard University Raman Lidar, 2nd Symposium on Lidar Atmospheric Applications, 85th AMS Annual Meeting, San Diego, CA (2006). (http://ams.confex.com/ams/pdfpapers/85650.pdf).

[3] D. N. Whiteman, B. Demoz, P. Di Girolamo, J. Comer, I. Veselovskii, K. Evans, Z. Wang, M. Cadirola, K. Rush, G. Schwemmer, B. Gentry, S. H. Melfi, B. Mielke, D. Venable, T. Van Hove, Atmos. Oc. Techn. **23**, 157-169 (2006).

[4] D. N. Whiteman, Appl. Opt. **42** (15), 2593-2608 (2003).

[5] D. N. Whiteman, Appl. Opt. **42** (15), 2571-2592 (2003).

[6] http://aeronet.gsfc.nasa.gov/

[7] D. N. Whiteman, F. Russo, B. Demoz, L. M. Miloshevich, I. Veselovskii, S. Hannon, Z. Wang, H. Vömel, F. Schmidlin, B. Lesht, P. J. Moore, A. S. Beebe, A. Gambacorta, C. Barnet, J.G.R., **111**, D09S09, doi 10.1029/2005JD006429, (2006).

[8] L. Miloshevich, H. Voemel, D. Whiteman, B. Lesht, F. J. Schmidlin, F. Russo, J. Geophys. Res. **111**, doi: 1029/2005JD006083 (2006).

[9] D. N. Whiteman, K. D. Evans, B. Demoz, et al., J. Geoph. Res. **106** (D6), 5211-5225 (2001).

[10] D. N. Whiteman, B. Demoz, Z. Wang, Geophys. Res. Lett. **31** (12), L12105 (2004).

[11] D. N. Whiteman, B. Demoz, P. Di Girolamo, J. Comer, I. Veselovskii, K. Evans, Z. Wang, D. Sabatino, G. Schwemmer, B. Gentry, R-F. Lin, A. Behrendt, V. Wulfmeyer, E. Browell, R. FerareE, S. Ismail, J. Wang, J. Atmos. Oc. Techn., **23**, 170-183 (2006).

*Corresponding author: madam@howard.edu